JM PAPERS

On the critical-throat boundary condition in quasi-one-dimensional linearised-Euler equation models

Frédéric Olivon[1,2] , Aurelien Genot[2] , Lionel Hirschberg[3] ,
Stéphane Moreau[4] and Avraham Hirschberg[5]

[1]DMPE, ONERA, Université Paris-Saclay, 91120 Palaiseau, France

[2]DMPE, ONERA, Université de Toulouse, 31000 Toulouse, France

[3]Engineering Fluid Dynamics, University of Twente, Enschede 7522 NB, The Netherlands

[4]Mechanical Engineering, Université de Sherbrooke, 2500 boulevard de l'Université, Sherbrooke J1K 2R1, QC, Canada

[5]Group Fluids and Flows, Dept. of Applied Physics and Science Education, Technische Universiteit Eindhoven, Eindhoven 5600 MB, The Netherlands

Corresponding author: Avraham Hirschberg, a.hirschberg@tue.nl

Based on the assumption of locally quasi-steady behaviour, Duran & Moreau (2013 *J. Fluid Mech.* **723**, 190–231), assumed that, at a critical nozzle throat, the fluctuations of the Mach number vanish for linear perturbations of a quasi-one-dimensional isentropic flow. This appears to be valid only in the quasi-steady-flow limit. Based on the analytical model of Marble & Candel (1977 *J. Sound Vib.* **55**, 225–243) an alternative boundary condition is obtained, which is valid for nozzle geometries with a finite limit of the second spatial derivative of the cross-section on the subsonic side of the throat. When the nozzle geometry does not satisfy this condition, the application of a quasi-one-dimensional theory becomes questionable. The consequences of this for the quasi-one-dimensional modelling of the acoustic response of choked nozzles are discussed for three specific nozzle geometries. Surprisingly, the relative error in the inlet nozzle admittance and acoustic wave transmission coefficient remains below a per cent, when the quasi-steady boundary condition is used at the throat. However, the prediction of the acoustic fluctuations assuming a quasi-steady critical-throat behaviour is incorrect, because the predicted acoustic field is singular at the throat.

Key words: aeroacoustics, gas dynamics

F. Olivon, A. Genot, L. Hirschberg, S. Moreau and A. Hirschberg

1. Introduction

The quasi-one-dimensional linearised-Euler equations provide an effective tool to analyse the response of choked nozzles, rocket engines or gas turbines to the passage of upstream-generated acoustic or entropic perturbations. Duran & Moreau (2013) provided an original analytical approach for the integration of one-dimensional equations and an extensive discussion of the literature available at that time. Their work has been quite influential, as evidenced by the high number of citations. Examples of recent notable publications citing Duran & Moreau (2013) are Magri (2017), Huet, Emmanuelli & Le Garrec (2020), Yeddula, Guzman-Inigo & Morgans (2022), Jain & Magri (2022) and Gentil *et al.* (2024). However, we have identified a problem with the locally quasi-steady boundary condition imposed by Duran & Moreau (2013) at the nozzle throat.

In this text, we propose a new alternative boundary condition for the choked-nozzle throat. This boundary condition is based on the idea of Crocco quoted by Tsien (1952) (in a footnote) that a physically relevant solution should not display a singularity. This idea was used by Marble & Candel (1977) to obtain an analytical solution for the acoustic response of a nozzle with the geometry of Tsien (1952). The geometry of Tsien (1952) is such that the time-averaged velocity profile in the nozzle is a linear function of the distance to the throat. Tsien (1952) and Marble & Candel (1977) show that, in that case, the general solution for the amplitude of an harmonically oscillating acoustic field can be expressed in terms of two hypergeometric functions of the distance to the throat. One of these hypergeometric functions is discarded because it has a leading-order term proportional to the inverse of the distance to the throat. This involves a singular behaviour at the throat. Moase, Brear & Manzie (2007) argue that the solution proposed by Marble & Candel (1977) is locally valid as long as the velocity gradient is uniform. In the present work the assumption of Crocco, that a non-singular solution prevails at the throat, is generalised to the case of more general nozzle profiles. The boundary condition is obtained as a combination of the equations of motion, from which a term is removed to impose a non-singular solution at the throat (Appendix A). Our analysis is limited to isentropic main-flow conditions of a perfect gas (an ideal gas with a constant specific heat ratio). The use of the proposed boundary condition is validated by comparison with a quasi-one-dimensional solution of the nonlinear Euler equations, solved by means of the CEDRE code (Refloch *et al.* (2011)). For the sake of efficiency the code is used with a single transversal mesh. Details of the numerical method used are provided in Appendix B.

A nozzle geometry for which experimental data on the inlet admittance Y are available (Bell, Daniel & Zinn (1973)) is considered. In addition, among the nozzles considered by Duran & Moreau (2013), the nozzle geometry proposed by Goh & Morgans (2011) has a discontinuity in the rate of change of the cross-section at the throat. The limitations of the quasi-one-dimensional model for such a geometry are highlighted. For this purpose both the original geometry of Goh & Morgans (2011) and a smoothed geometry obtained by mirroring the upstream geometry with respect to the throat (Appendix C) are considered. The limitations of quasi-one-dimensional models due to two-dimensional effects as discussed by Emmanuelli *et al.* (2020) for entropy sound are ignored.

2. Upstream acoustic boundary condition at the critical nozzle throat

At the quasi-steady and low-frequency limit, the nozzle throat remains choked when subjected to perturbations, and the perturbation M' of the Mach number M vanishes at any position up to the choked throat. This is a direct consequence of the fact that, for an isentropic quasi-one-dimensional flow, the Mach number is only a function of A_*/A, the

ratio of the throat cross-section A_* and the local channel cross-section A. Indeed, for an ideal gas with constant heat capacity ratio $\gamma \equiv c_p/c_v$, this ratio is (Shapiro (1953))

$$\frac{A_*}{A} = M \left(\frac{\gamma + 1}{2 + (\gamma - 1)M^2} \right)^{\frac{\gamma+1}{2(\gamma-1)}}, \tag{2.1}$$

where the subscript $()_*$ refers to the conditions at the choked-nozzle throat ($M_* = 1$). As there are no perturbations of the geometry ($A' = 0$) the linearisation of this equation implies $M' = 0$, at any position upstream of the critical nozzle throat, in the quasi-steady limit. This low-frequency approximation was introduced by Tsien (1952) and Marble & Candel (1977).

The analysis of Stow, Dowling & Hynes (2002) suggests that, up to the first order in the frequency, the quasi-steady boundary condition $M'_* = 0$ remains valid at the throat. Duran & Moreau (2013) assumed that one can always consider a narrow region around the critical throat for which a quasi-steady approximation is valid, because the said region is small compared with the wavelength of perturbations. This would imply the validity of the condition $M'_* = 0$ for any frequency. However, this is in fact not correct. In the following, a correction for the critical-throat upstream boundary condition is proposed. Moreover, some limitations of the quasi-one-dimensional theory are discussed.

Tsien (1952) considered a nozzle geometry such that the steady-flow longitudinal-velocity gradient ($d\bar{u}/dx$) is constant within the nozzle. Using the nozzle geometry of Tsien (1952), Marble & Candel (1977) obtained an exact solution for the linear perturbations of a quasi-one-dimensional flow through a choked nozzle. In their case, the constant velocity gradient in the nozzle is $d\bar{u}/dx = (d\bar{u}/dx)_* = c_*/x_*$, with c_* the critical speed of sound and x_* the distance between the throat and a point at which the extrapolated linear velocity $\bar{u}(x) = c_*(x/x_*)$ vanishes. For an inlet Mach number M_i and corresponding speed of sound c_i one has $c_*/c_i = \sqrt{(\gamma + 1)/(2 + (\gamma - 1)M_i^2)}$. Using the continuity of the normalised amplitude of the pressure fluctuations $P = \hat{p}/(\gamma \bar{p})$ and its derivatives, the boundary condition just upstream from the choked nozzle found by substituting ($x/x_* = 1$) in (45) of Marble & Candel (1977) (or (2.24c) of Moase *et al.* (2007)) is

$$(2 + i\hat{\Omega})U_* = (\gamma - 1 + i\hat{\Omega})P_* + \sigma_*, \tag{2.2}$$

where the dimensionless velocity U, pressure P and entropy σ are defined as

$$U = \left(\frac{\hat{u}}{\bar{u}} \right); \quad P = \left(\frac{\hat{p}}{\gamma \bar{p}} \right); \quad \sigma = \left(\frac{\hat{s}}{c_p} \right), \tag{2.3}$$

and the dimensionless frequency $\hat{\Omega}$ as

$$\hat{\Omega} \equiv \frac{2\pi f}{(d\bar{u}/dx)_*}, \tag{2.4}$$

where $\hat{u}$, $\hat{p}$ and $\hat{s}$ are the amplitudes of the harmonic oscillations of frequency f in axial velocity u, pressure p and entropy s, respectively ($y = \bar{y} + y' = \bar{y} + \hat{y} \exp[+i\omega t]$, with $\bar{y}$ the time-averaged values of $y = u$, p or s). Details of the derivation of this boundary condition are provided in Appendix A.

It is proposed that, as long as the quasi-one-dimensional assumption remains valid, the boundary condition given in (2.2) can be generalised by incorporating (2.4), where the local velocity gradient $(d\bar{u}/dx)_*$ at the throat is used.

For isentropic flow the amplitude fluctuations of the Mach number at the critical throat are then given by

$$\hat{M}_* = \left(\frac{\gamma - 1 + i\hat{\Omega}}{2 + i\hat{\Omega}} - \frac{\gamma - 1}{2} \right) P_*. \tag{2.5}$$

It should be noted that the theory of Marble & Candel (1977) relies on a quasi-one-dimensional approximation. We generalised this notion and, in the following, apply it to a sufficiently smooth nozzle profile.

The proposed generalised boundary condition just upstream from the choked throat, within a quasi-one-dimensional framework, exhibits meaningful asymptotic behaviour in both the low- and high-frequency limits.

At low frequencies, $\hat{\Omega} < 1$, (2.2) yields

$$U_* = \left(\frac{\gamma - 1}{2} + i\hat{\Omega} \frac{(\gamma + 1)}{4} \right) P_* + \frac{\sigma_*}{2} \left(1 - i\frac{\hat{\Omega}}{2} \right) + O(\hat{\Omega}^2), \tag{2.6}$$

which corresponds to the first-order correction to the quasi-static condition $M'_* = 0$.

At high frequencies, $\hat{\Omega} >> 1$, one finds

$$U_* = P_* \left(1 - i\frac{\gamma + 1}{\hat{\Omega}} \right) - i\frac{\sigma_*}{\hat{\Omega}} + O(\hat{\Omega}^{-2}), \tag{2.7}$$

which is a first-order correction to the simple-wave downstream-radiation condition in a tube of uniform cross-section: $p'_* = (\bar{\rho}\bar{c}u')_*$ (at the throat one has $(dA/dx)_* = 0$).

It is noteworthy that the influence of entropy fluctuations on the boundary condition at the critical throat becomes negligible at very high frequencies (for an isentropic main steady flow).

For a given cross-sectional area $A(x)$, assuming a quasi-one-dimensional isentropic steady reference flow with constant γ, the rule of l'Hopital to determine the critical flow behaviour (Shapiro 1953, § 8.10) yields

$$\left(\frac{d\bar{u}}{dx} \right)_* = c_* \sqrt{\frac{1}{(\gamma + 1)A_*} \left(\frac{d^2 A}{dx^2} \right)_*}. \tag{2.8}$$

Hence, as long as the second derivative d^2A/dx^2 exists at the critical throat, which is characterised by $(dA/dx)_* = 0$, the boundary condition ((2.2)) can be used. When $(dA/dx)_*$ is discontinuous, as for the nozzle geometry proposed by Goh & Morgans (2011), the boundary condition will be applied in the limit approaching the throat from the upstream (subsonic) side.

3. Validation and limits of the quasi-one-dimensional model

To validate the proposed model numerical integration of the nonlinear Euler equations for quasi-one-dimensional flows was done using the unstructured computational fluid dynamics (CFD) code CEDRE (Refloch *et al.* (2011)). Details of this model and information concerning numerical aspects are provided in Appendix B.

Using CEDRE, isentropic harmonic pressure fluctuations were imposed at the nozzle inlet with an amplitude of $|p'|/(\gamma\bar{p}) = 1\%$. For the CEDRE-model results, both the steady-flow velocity gradient $(d\bar{u}/dx)_*$ and the amplitude $\hat{M}_*$ of the Mach number fluctuations are numerically extracted by approaching the throat from the subsonic side.
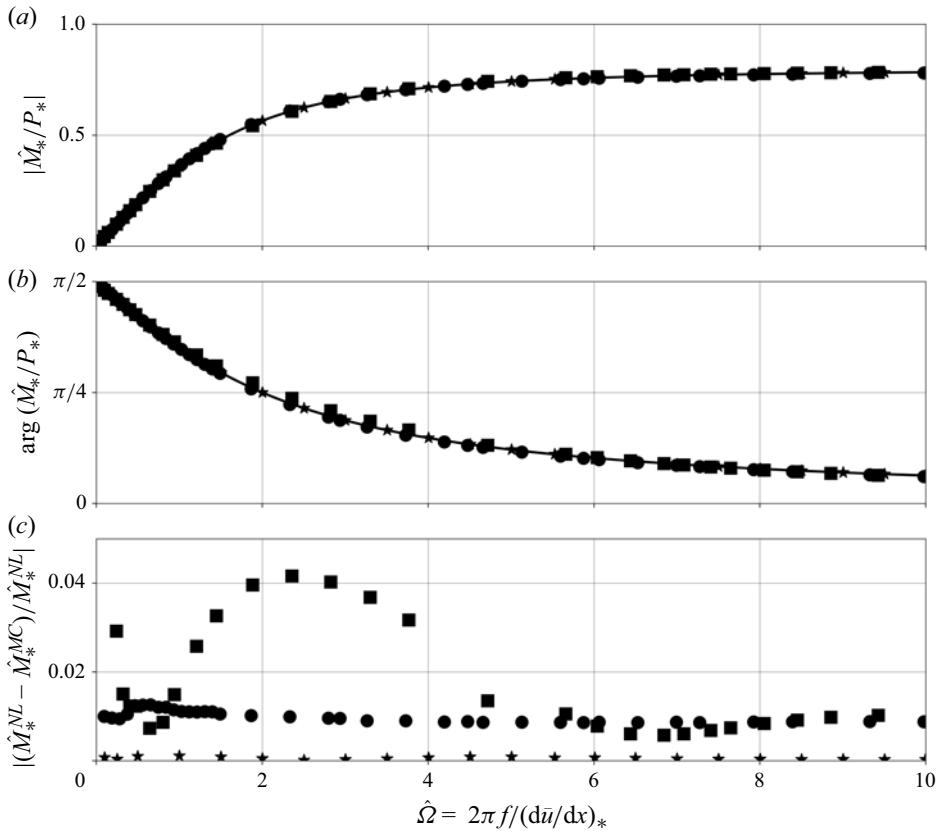
Figure 1. Modulus $|\hat{M}_*/P_*|$ (*a*) phase angle $\arg(\hat{M}_*/P_*)$ (*b*) of the normalised critical Mach number fluctuations and relative deviation $|(\hat{M}_*^{NL} - \hat{M}_*^{MC})/\hat{M}_*^{NL}|$ (*c*) between numerical ($\hat{M}_*^{NL}$, Refloch *et al.* (2011)) and analytical ($\hat{M}_*^{MC}$, (2.5)) results (——) as a function of the dimensionless frequency $\hat{\Omega} = 2\pi f/(\mathrm{d}\bar{u}/\mathrm{d}x)_*$ for three nozzle geometries the 'smoothed' nozzle of Bell *et al.* (1973) (●), the 'smoothed' nozzle of Goh & Morgans (2011) (⋆) and the original nozzle of Goh & Morgans (2011) with discontinuous $\mathrm{d}A/\mathrm{d}x$ at the throat (■).

The influence of nonlinear effects, as accounted for in the CEDRE model, was assessed by performing simulations with varying input amplitudes ($|p'|/(\gamma\,\bar{p}) = 0.1\,\%-2\,\%$). The results indicate that nonlinearities contribute less than 0.1 % to the overall deviation.

In figure 1 the evolution of the normalised fluctuation amplitude $|\hat{M}_*/P_*|$ of the critical Mach number is shown as a function of the dimensionless frequency for both the modified analytical model (( )^{MC},——) and the nonlinear (CEDRE) results (( )^{NL}).

A fair agreement is found (within 1 %) between both approaches for the nozzle of Bell *et al.* (1973) (●) and one order of magnitude better for the smoothed nozzle of Goh & Morgans (2011) (⋆), both geometries have well-defined $(\mathrm{d}^2A/\mathrm{d}x^2)_*$ (see Appendix C). While deviations of the order of 1 % remain for the nozzle of Bell *et al.* (1973), it is clear that the proposed generalised boundary condition (2.2) provides a much better prediction of the critical-throat behaviour than the quasi-steady assumption $\hat{M}_* = 0$. This deviation was found to be independent of the chosen numerical parameters (see Appendix B).

In the following the original nozzle geometry of Goh & Morgans (2011) (with a discontinuity in $(\mathrm{d}A/\mathrm{d}x)$ at the throat, Appendix C) will be considered (■). The definition

of $\hat{\Omega}$ and the boundary condition (2.2) are assumed to be valid as long as $(\mathrm{d}\bar{u}/\mathrm{d}x)_*$ has a well-defined finite value, to wit, when the throat is approached from the subsonic side ($M \leqslant 1$). The limit of $(\mathrm{d}^2\mathrm{A}/\mathrm{d}x^2)_* = \lim_{x\uparrow x_*}(\mathrm{d}^2\mathrm{A}/\mathrm{d}x^2)$ on the subsonic side of the throat is used to calculate $(\mathrm{d}\bar{u}/\mathrm{d}x)_*$ by means of (2.8). In this case, we posit that, because of the deviation from quasi-one-dimensional behaviour, a one-dimensional model for the behaviour of the actual nozzle should at the throat have a second derivative of the order of magnitude 1; viz., $(\mathrm{d}^2\mathrm{A}/\mathrm{d}x^2)_* = O(1)$. Moreover, we submit that the exact value of $(\mathrm{d}^2\mathrm{A}/\mathrm{d}x^2)_*$ that should be used depends on the actual shape of the channel in the throat (two-dimensional planar or axisymmetric flow). This proposed geometric correction will hereafter be referred to as smoothing.

However, if one elects to not apply the above-suggested correction for quasi-one-dimensional geometries, and one applies the quasi-one-dimensional theory to the original geometry proposed by Goh & Morgans (2011), some numerical problems arise. One observes in figure 1 a larger deviation for the original geometry of Goh & Morgans (2011) compared with the smoothed one.

The deviation is at least partially due to a problem in application of the CEDRE numerical scheme (used with a single lateral mesh) to a flow with discontinuity of $(\mathrm{d}\mathrm{A}/\mathrm{d}x)$ at the throat. There is a significant difference between the analytical value of $(\mathrm{d}\bar{u}/\mathrm{d}x)_*$ (2.8) and the value calculated numerically. This relative difference is estimated to 1×10^{-2} for the considered geometries. This results into a systematic error in the calculation of $\hat{\Omega}$ by means of (2.4).

4. Influence of the boundary condition on the acoustic pressure distribution

In this section, the influence of the proposed critical-throat boundary condition on the shape of the longitudinal distribution of the pressure fluctuations is discussed. Use of a quasi-one-dimensional linearised-Euler model incorporating (2.2) as the boundary condition at the throat or the quasi-steady assumption $M'_* = 0$ of Duran & Moreau (2013) was made to investigate this. Typical results for the nozzle of Bell *et al.* (1973) are shown in figure 2. One observes for the quasi-steady boundary condition $M'_* = 0$ a discontinuity of $|\hat{p}|$ at the throat $x = x_*$. The above-described observation led us to examine the boundary condition at the choked throat more carefully. This discontinuity is eliminated when the proposed boundary condition (2.2) is applied.

5. Acoustic reflection and transmission coefficients

In figure 3 the acoustic-reflection coefficient R_a normalised by the quasi-steady-state value $(2 - (\gamma - 1)\bar{M}_i)/(2 + (\gamma - 1)\bar{M}_i)$ (Marble & Candel (1977)) as a function of the dimensionless frequency $\hat{\Omega} = 2\pi f/(\mathrm{d}\bar{u}/\mathrm{d}x)_*$ is shown. Results obtained using both the CEDRE model and the quasi-one-dimensional linear model are provided for the three above-considered geometries. For the linear model of the nozzle of Goh & Morgans (2011) the value of $(\mathrm{d}\bar{u}/\mathrm{d}x)_*$ calculated analytically, just upstream from the throat, by means of (2.8) is used. The proposed acoustic boundary condition is used to close the linear model. An excellent agreement is found between linear analytical and nonlinear numerical results for the smoothed nozzle geometry. Some differences are observed for the original geometry of Goh & Morgans (2011). As noted above, calculating numerically the gradient $(\mathrm{d}\bar{u}/\mathrm{d}x)_*$ poses some problems for the original discontinuous nozzle geometry of Goh & Morgans (2011). To assess the impact of the proposed boundary condition relative to the commonly used quasi-steady critical Mach number model $M'_* = 0$, the relative difference in the linear model results is evaluated using two different
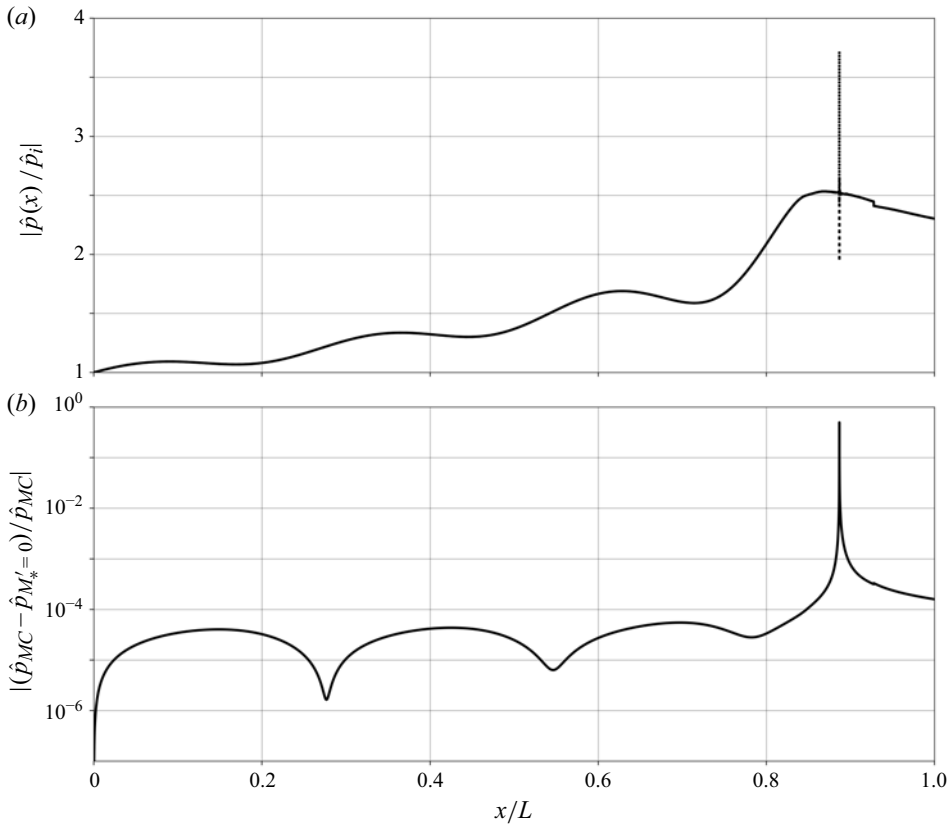
Figure 2. Modulus (*a*) of the acoustic pressure, $|\hat{p}(x)/\hat{p}_i|$, as a function of the position along the *x*-axis, for the dimensionless frequency $\hat{\Omega} = 2.06$ (nozzle of Bell *et al.* (1973)). The linear analytical model is provided for two critical-throat boundary conditions: respectively $(\hat{M}_*)_{MC}$ (2.2), —) and locally quasi-steady-flow condition $M'_* = 0$ (⋯⋯). The absolute relative difference is shown in the graph (*b*).

critical boundary conditions: MC, corresponding to $(\hat{M}_*)_{MC}$ (2.2), and the quasi-steady assumption $M'_* = 0$. As expected, at low frequencies the difference between the two boundary conditions is minimal. However, this difference increases with frequency, reaching 2×10^{-2} for the geometry of Bell *et al.* (1973) and 3×10^{-3} for the two geometries of Goh & Morgans (2011).

In figure 4, the acoustic transmission coefficient T_a is plotted as a function of the dimensionless frequency $\hat{\Omega} = 2\pi f/(\mathrm{d}\bar{u}/\mathrm{d}x)_*$. Results obtained from both the CEDRE simulations and the quasi-one-dimensional linear model are shown for the three nozzle geometries previously considered. The proposed boundary condition (2.2) is used to close the quasi-one-dimensional linear model. Excellent agreement is observed between the linear analytical and nonlinear numerical results for both the 'smoothed' and original nozzle geometries of Goh & Morgans (2011). For the nozzle of Bell *et al.* (1973), a maximum deviation of 3×10^{-1} between nonlinear and linear results is observed at very high frequencies, while at low frequencies ($\hat{\Omega} < 1$), a fair agreement is maintained.

To evaluate the impact of the proposed boundary condition compared with the quasi-steady critical Mach number model $M'_* = 0$, the relative difference in the acoustic transmission coefficient T_a predicted by the linear model is computed using both boundary
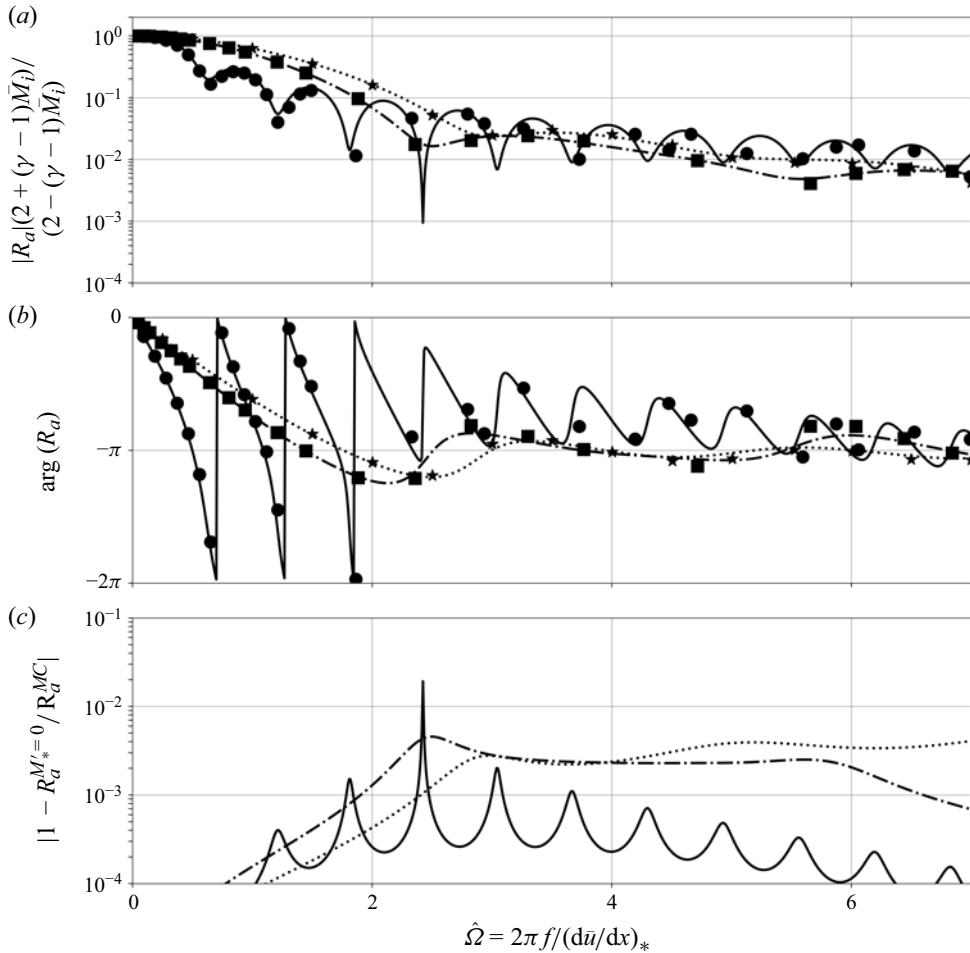
Figure 3. Modulus $|R_a|(2 + (\gamma - 1)\bar{M}_i)/(2 - (\gamma - 1)\bar{M}_i)$ (a) and phase angle $\arg(R_a)$ (b) of the CEDRE acoustic-reflection coefficient as a function of the dimensionless frequency $\hat{\Omega} = 2\pi f/(\mathrm{d}\bar{u}/\mathrm{d}x)_*$ for three nozzle geometries (Bell *et al.* 1973 (●), original Goh & Morgans 2011(■) and 'smoothed' Goh & Morgans 2011 (⋆)). Results obtained by means of the quasi-one-dimensional acoustic model are also shown (Bell *et al.* 1973 (——), original Goh & Morgans 2011 (-·-)) and 'smoothed' Goh & Morgans 2011 (····)). The absolute relative difference $|1 - R_a^{M'_* = 0}/R_a^{MC}|$ (c) between the quasi-one-dimensional linear model using two different boundary conditions at the throat (respectively, R_a^{MC} for $(\hat{M}_*)_{MC}$ (2.2) and $R_a^{M'_* = 0}$ for $M'_* = 0$) is shown in the lower graph.

conditions: the proposed model (denoted MC, (2.2)) and the quasi-steady assumption $M'_* = 0$. As expected, the difference between the two boundary conditions is negligible at low frequencies, with relative deviations below 1×10^{-5}. However, this difference increases with frequency, reaching 1×10^{-4} for the two geometries of Goh & Morgans (2011). A similar behaviour is observed for the nozzle of Bell *et al.* (1973), with a maximum deviation of 2×10^{-4}.

The results of Bell *et al.* (1973) for the admittance (Y) defined as the inverse of the impedance (Z)

$$Y = \frac{1}{Z} = \rho c \left.\frac{\hat{u}}{\hat{p}}\right|_i = \left.\frac{MU}{P}\right|_i = \frac{1 - R_a}{1 + R_a}, \tag{5.1}$$
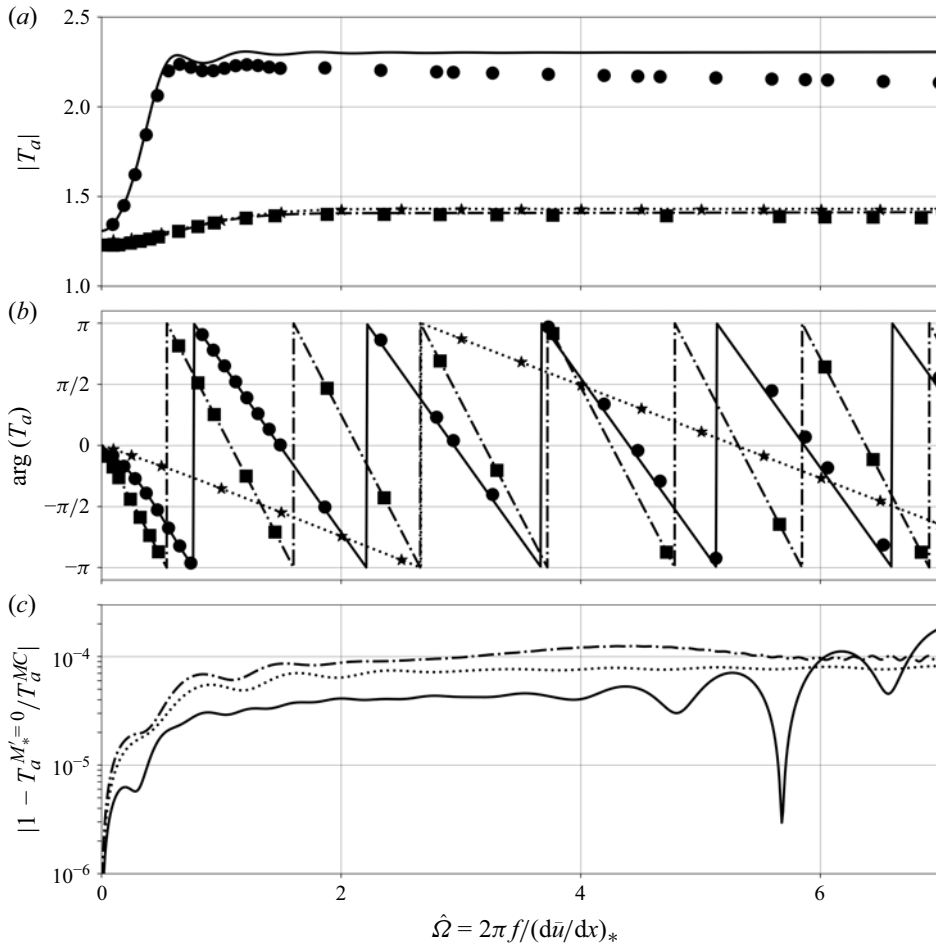
Figure 4. Modulus $|T_a|$ (a) and phase angle $\arg(T_a)$ (b) of the CEDRE acoustic-reflection coefficient as a function of the dimensionless frequency $\hat{\Omega} = 2\pi f/(\mathrm{d}\bar{u}/\mathrm{d}x)_*$ for three nozzle geometries (Bell *et al.* 1973 ($\bullet$), original Goh & Morgans 2011 ($\blacksquare$) and 'smoothed' Goh & Morgans 2011 ($\star$)). Results obtained by means of the quasi-one-dimensional acoustic model are also shown (Bell *et al.* (1973) (——), original Goh & Morgans (2011) (– · –)) and 'smoothed' Goh & Morgans (2011) (· · · · ·). The absolute relative difference $|1 - T_a^{M'_*=0}/T_a^{MC}|$ (c) between the quasi-one-dimensional linear model using two different boundary conditions at the throat (respectively, T_a^{MC} for $(\hat{M}_*)_{MC}$ (2.2) and $T_a^{M'_*=0}$ for $M'_* = 0$) is shown in the lower graph.

are shown in figure 5 and compared with results obtained with the CEDRE model and quasi-one-dimensional model. At low frequencies $\hat{\Omega} < 1$ the difference between Y_{MC} (calculated with (2.2)) and $Y_{M'_*=0}$ is negligible because one approaches the quasi-steady behaviour $M'_* = 0$. At high frequencies $\hat{\Omega} > 5$ the error is less than 0.1 %. For intermediate frequencies ($1 < \hat{\Omega} < 5$), one observes a few peaks in the error that reach the order of a few per cent.

As the error in predicted reflection and transmission coefficients due to the use of the quasi-stationary boundary condition $(M')_* = 0$ is small, the global conclusions obtained by Duran & Moreau (2013) are correct. While for the isentropic flow conditions
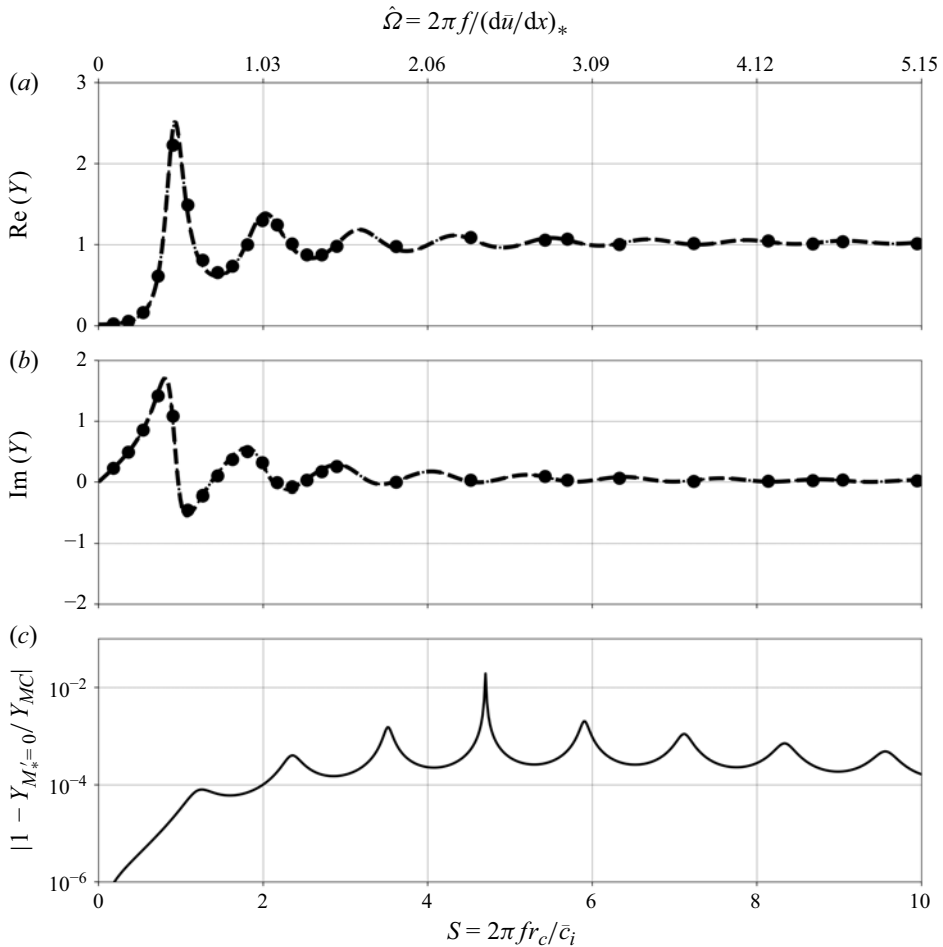
$$\hat{\Omega} = 2\pi f/(d\bar{u}/dx)_*$$

Figure 5. Comparison of acoustic admittance (Y) for the geometry of Bell *et al.* (1973) calculated with CEDRE (●) and with the quasi-one-dimensional linear model using two different boundary conditions at the throat (respectively, Y_{MC} for $(\hat{M}_*)_{MC}$ (2.2), (······) and $Y_{M'_*=0}$ for $M'_* = 0$) (- -). Real (*a*) and imaginary (*b*) parts of the acoustic admittance are presented as function of the dimensionless frequency S (using the notation of Bell *et al.* (1973)). The corresponding alternative dimensionless frequency $\hat{\Omega} = 2\pi f/(d\bar{u}/dx)_*$ is indicated on top of the graph. The absolute value of the relative difference $|\epsilon| = |(Y_{MC} - Y_{M'_*=0})/Y_{MC}|$ (*c*) is shown in the lower graph.

considered, we only observe minor errors in the reflection and transmission coefficients, the solution with a singularity at the throat remains physically wrong.

6. Conclusions

The quasi-one-dimensional linearised-Euler equations can be integrated for isentropic steady main flow through a choked nozzle by using the proposed boundary condition at the critical throat (2.2). This is a generalisation of Marble & Candel's (1977) boundary condition. While Marble & Candel (1977) assume a constant velocity gradient $d\bar{u}/dx$ within the nozzle, the proposed theory only assumes the continuity at the throat of the slope dA/dx and second derivative d^2A/dx^2 for the subsonic part of the nozzle cross-section $A(x)$.

1019 A4-10

We find that when there is a discontinuity in dA/dx, as in the nozzle geometry proposed by Goh & Morgans (2011), the quasi-one-dimensional approximation must be used with care. Firstly, the quasi-one-dimensional assumption with a discontinuity in the slope dA/dx may not accurately represent the actual flow. Secondly, the discontinuity, combined with the numerical methodology used in CEDRE (single lateral mesh, implicit time integration, spatial discretisation methods adapted to complex flows and unstructured meshes), may result in greater discrepancies between the linear model and CEDRE solutions.

Moreover, when the quasi-steady assumption $M'_* = 0$ is used, the predicted amplitude of acoustic fluctuation shows a singularity at the throat, which is not observed in nonlinear quasi-one dimensional numerical simulations using CEDRE. However, the prediction of the inlet reflection coefficient, admittance and transmission coefficient do not seem to be significantly affected in the case of the chosen geometries, which explains the satisfactory results obtained by Duran & Moreau (2013). For more complex flows, such as non-isentropic heated flows (e.g. thermally choked nozzles), the use of the proposed boundary condition might be essential to accurately describe the acoustic behaviour.

Appendix A. Generalised critical-throat boundary condition

A.1. *Flow motion model*

For an ideal gas, assuming no losses due to viscosity, thermal diffusion or external force fields, the standard quasi-one-dimensional equations for mass, momentum and energy conservation are expressed as follows:

$$\begin{cases} \dfrac{D\rho}{Dt} + \rho\dfrac{\partial u}{\partial x} + \rho u\alpha = 0, \\[2mm] \dfrac{Du}{Dt} + \dfrac{1}{\rho}\dfrac{\partial p}{\partial x} = 0, \\[2mm] \dfrac{Dp}{Dt} - c^2\dfrac{D\rho}{Dt} = 0, \end{cases} \tag{A1}$$

where $D/Dt = \partial/\partial t + u\,\partial/\partial x$ is the material derivative, ρ is the density, u is the longitudinal velocity, $\alpha = (dA/dx)/A$ is the relative variation of the nozzle cross-sectional area A, p is the static pressure, c is the speed of sound and $\gamma \equiv c_p/c_v$ is the ratio of specific heats at constant pressure c_p and constant volume c_v. For clarity and conciseness, the system of (A1) will hereafter be referred to as the quasi-one-dimensional Euler equations.

To close the quasi-one-dimensional Euler equations (A1), the ideal gas law is used

$$p = \rho r T, \tag{A2}$$

where T is the static temperature, $r = \mathcal{R}/\mathcal{W}$ is the specific gas constant, with $\mathcal{R} = 8.3145\,\mathrm{J\,mol^{-1}\,K^{-1}}$ the universal gas constant, and $\mathcal{W}$ the molar mass of the gas.

The gas considered here is air, described as an ideal gas with a specific isobaric heat capacity c_p independent of the temperature and prescribed as constant.

A.2. *Linearised-Euler equation system*

To study the propagation of acoustic waves through a nozzle with non-uniform steady flow-field, quasi-one-dimensional Euler equations (A1) are linearised using the perturbation convention $y(x, t) = \bar{y}(x) + y'(x, t)$, where $\bar{y}$ denotes the steady component and y' the small perturbation of $y = [\rho, u, p, T, c]$. Neglecting second-order perturbations and introducing the normalised quantities $D' = \rho'/\bar{\rho}$, $U' = u'/\bar{u}$, $P' = p'/(\gamma \bar{p})$ yields the following linearised system of differential equations:

$$
\begin{cases}
\dfrac{\partial D'}{\partial t} + \bar{u}\dfrac{\partial}{\partial x}\left(U' + D'\right) = 0, \\[3mm]
\dfrac{\partial U'}{\partial t} + \bar{u}\dfrac{\partial U'}{\partial x} + \dfrac{\bar{c}^2}{\bar{u}}\dfrac{\partial P'}{\partial x} + \dfrac{\mathrm{d}\bar{u}}{\mathrm{d}x}\left(2\,U' - \gamma\,P' + D'\right) = 0, \\[3mm]
\dfrac{\partial P'}{\partial t} + \bar{u}\dfrac{\partial}{\partial x}\left(U' + P'\right) = 0.
\end{cases}
\tag{A3}
$$

A.3. *Critical-throat boundary condition*

To obtain the quasi-one-dimensional critical-throat boundary condition model for an isentropic choked flow nozzle, the quasi-one-dimensional linearised-Euler equations (A3) are considered.

The steady-flow velocity profile, $\bar{u}(x)$, is locally approximated at the throat as $\bar{u}(\tilde{x}) = (\mathrm{d}\bar{u}/\mathrm{d}x)_* \tilde{x}$, where $(\mathrm{d}\bar{u}/\mathrm{d}x)_*$ denotes the velocity gradient at the critical throat. The origin of the coordinate $\tilde{x}$ is chosen such that the extrapolated velocity profile $\bar{u}(\tilde{x})$ vanishes at $\tilde{x} = 0$. Hence, the throat position is $\tilde{x}_* = \bar{c}_*/(\mathrm{d}\bar{u}_*/\mathrm{d}x)_*$. Based on this definition, the following time–space transformation is introduced as performed by Marble & Candel (1977):

$$
\tau = \frac{\bar{c}_*}{\tilde{x}_*}t; \quad \xi = \left(\frac{\tilde{x}}{\tilde{x}_*}\right)^2.
\tag{A4}
$$

The linearised momentum and total energy Euler equations (A3) can be rewritten using the time–space transformation as follows:

$$
\begin{cases}
\dfrac{\partial U'}{\partial \tau} + 2\xi\dfrac{\partial U'}{\partial \xi} + 2\dfrac{\bar{c}^2}{\bar{c}_*^2}\dfrac{\partial P'}{\partial \xi} + 2\,U' - \gamma\,P' + D' = 0, \\[3mm]
\dfrac{\partial P'}{\partial \tau} + 2\xi\dfrac{\partial}{\partial \xi}\left(U' + P'\right) = 0.
\end{cases}
\tag{A5}
$$

Introducing the dimensionless frequency $\hat{\Omega} \equiv 2\pi f/(\mathrm{d}\bar{u}/\mathrm{d}x)_*$, the system (A5) is further expressed in the frequency domain. Applying the Fourier transform, with the convention $y(\xi, \tau) = \hat{y}(\xi)\exp(+\mathrm{i}\hat{\Omega}\tau)$, to the variables $D = \hat{\rho}/\bar{\rho}$, $U = \hat{u}/\bar{u}$, and $P = \hat{p}/(\gamma\bar{p})$, the resulting system of equations becomes:

$$
\begin{cases}
2\xi\dfrac{\mathrm{d}U}{\mathrm{d}\xi} + 2\dfrac{\bar{c}^2}{\bar{c}_*^2}\dfrac{\mathrm{d}P}{\mathrm{d}\xi} + \left(2 + \mathrm{i}\hat{\Omega}\right)U - \gamma\,P + D = 0 \\[3mm]
2\xi\dfrac{\mathrm{d}U}{\mathrm{d}\xi} + 2\xi\dfrac{\mathrm{d}P}{\mathrm{d}\xi} + \mathrm{i}\hat{\Omega}\,P = 0
\end{cases}
\tag{A6}
$$

Subtracting the momentum equation from the energy equation yields

$$2\left(\xi - \frac{\bar{c}^2}{\bar{c}_*^2}\right)\frac{\mathrm{d}P}{\mathrm{d}\xi} - \left(2 + \mathrm{i}\hat{\Omega}\right)U + \left(\gamma + \mathrm{i}\hat{\Omega}\right)P - D = 0. \tag{A7}$$

This equation is now evaluated at the steady critical-throat position. The assumption of Tsien (1952), as proposed by Crocco, is used such that $\widehat{U}$, $\widehat{P}$ and $\widehat{D}$, as well as their derivatives, are continuous at the critical-throat location. It is further assumed that none of the derivatives are proportional to $1/(1 - \xi)$, as such a condition would lead to a singularity at the critical throat. Under these assumptions, and because at the throat $\xi = 1$ and $\bar{c}_* = \bar{c}$, the term proportional to $(\mathrm{d}P/\mathrm{d}\xi)_*$ vanishes and the boundary condition at the critical-throat position becomes

$$\left(2 + \mathrm{i}\hat{\Omega}\right)U_* = \left(\gamma + \mathrm{i}\hat{\Omega}\right)P_* - D_*. \tag{A8}$$

For a mono-species gas, the linearised Gibbs equation provided a relation between entropy, pressure and density fluctuations

$$D_* = \sigma_* - P_*. \tag{A9}$$

Finally, the entropy-based form of the boundary condition writes

$$\left(2 + \mathrm{i}\hat{\Omega}\right)U_* = \left(\gamma - 1 + \mathrm{i}\hat{\Omega}\right)P_* + \sigma_*. \tag{A10}$$

Appendix B. The CEDRE numerical model and integration linear model

The Euler equations are considered for a calorically perfect, ideal gas (Duran & Moreau (2013)). The numerical simulations are performed using the ONERA CFD code CEDRE (Refloch *et al.* (2011)). The computational set-up consists of a two-dimensional domain discretised with $\Delta x/L = 5 \times 10^{-5}$ for each geometry. This resolution ensures adequate spatial discretisation of acoustic waves, providing at least 50 points per wavelength for frequencies below 6000 Hz.

Since the flow is assumed to be purely longitudinal, only one cell is used to discretise the transverse direction. This single lateral mesh is numerically very efficient but might not be an optimal use of the code. Spatial discretisation employs a second-order multi-slope Monotonic Upstream-centered Scheme for Conservation Laws interpolation method with an Harten-Lax-van Leer-Contact solver (Le Touze, Murrone & Guillard (2015)), while temporal integration is carried out using an implicit second-order Runge–Kutta scheme with a time step of $\Delta t = 5 \times 10^{-7}$ s, ensuring a Courant–Friedrichs–Lewy number of $\bar{u}_i \Delta t/\Delta x = 0.27$, with $\bar{u}_i$ the inlet steady flow-field velocity.

Unsteady solutions corresponding to acoustic forcing are obtained using a modulated post-processing time step based on the inlet forcing frequency. To ensure satisfactory temporal resolution, 50 periods are simulated, with 100 points per period selected for data storage. Spectral analysis (fast Fourier transform) is performed on the last 35 periods to ensure that transient phenomena are excluded.

For mono-harmonic isentropic acoustic forcing, entropy injection is eliminated from the flow by imposing the following two inlet-boundary conditions:

$$\begin{cases} p_i(t) &= \bar{p}_i \left(1 + \eta \sin(2\pi f t)\right), \\ T_i(t) &= \bar{T}_i \left(1 + (\gamma - 1)\dfrac{p_i(t) - \bar{p}_i}{\gamma \bar{p}_i}\right), \end{cases} \tag{B1}$$

where f is the chosen frequency, and η is set to ensure that the normalised pressure fluctuation amplitude is $|p_i'|/(\gamma \bar{p}_i) = 1\%$. A supersonic boundary condition is applied

at the outlet of the geometry, allowing for the evacuation of acoustic waves. Simulations with four levels of grid refinement ($\Delta x/L = 5 \times 10^{-4}$, 1×10^{-4}, 5×10^{-5} and 1×10^{-5}, where L is the length of the nozzle) and three time steps ($\Delta t = 1 \times 10^{-6}$, 5×10^{-7} and 1×10^{-7}) confirm the independence of the results, indicating that the discretisation error in the presented simulations is negligible. The validation of the mesh independence is performed by comparing the steady velocity gradient $(\mathrm{d}\bar{u}/\mathrm{d}x)_*$ at the critical throat. One finds a maximum relative deviation of 9×10^{-3} in $(\mathrm{d}\bar{u}/\mathrm{d}x)_*$ estimated with CEDRE compared with the one-dimensional analytical solution (2.8), for the original nozzle geometry of Goh & Morgans (2011). The validation of the chosen time step independence is performed by comparing the normalised pressure fluctuations, $p'/(\gamma \bar{p})$, for each nozzle geometry for an acoustic forcing of $\hat{\Omega} = 10$. A maximum relative deviation of 6×10^{-4} is found.

The linearised quasi-one-dimensional Euler equation system (Marble & Candel (1977)) is solved for velocity, pressure and density fluctuations using an iterative shooting method, starting from the inlet-boundary conditions. Spatial integration is performed with an explicit fourth-order Runge–Kutta scheme. Integration with lower-order schemes and different discretisations gave the same results, confirming the numerical convergence of the results.

Appendix C. Nozzle geometries

The two-dimensional planar nozzle geometry studied by Goh & Morgans (2011) is defined as follows:

$$\frac{A(\xi)}{A_*} = \begin{cases} \frac{1}{2}\left(\frac{A_i}{A_*} - 1\right)\left(\cos\left(\pi\frac{\xi}{\xi_*}\right) + 1\right), & \xi \in [0, \xi_*], \\ 1 + \left(\frac{A_o}{A_*} - 1\right)\frac{\xi - \xi_*}{1 - \xi_*}, & \xi \in [\xi_*, 1], \end{cases} \tag{C1}$$

where $A(\xi)$ is the nozzle cross-sectional area at position $\xi = x/L$.

This geometry is fully defined using the normalised inlet $()_i$ and outlet $()_o$ sections, A_i/A_* and A_o/A_*, as well as the normalised critical-throat position $\xi_* = (x_*/L) = 0.15$. In this study, the inlet and outlet Mach numbers are prescribed as $M_i = 0.29$ and $M_o = 1.5$, respectively. The corresponding normalised inlet and outlet areas, A_i/A_* and A_o/A_*, are obtained using the following isentropic area–Mach number relation (2.1). A smooth version of this geometry is obtained by mirroring the subsonic geometry with respect to the throat.

The subsonic part of the cylindrical symmetric nozzle of Bell *et al.* (1973) has an inlet radius r_c. Its longitudinal cross-section consists of three sections: a circular arc of radius r_{cc} and angle θ, a conical section with the same angle θ and another circular arc with the same radius r_{cc} and angle θ

$$r(x) = \begin{cases} r_c - r_{cc}\left[1 - \cos\left(\arcsin\left(\frac{x}{r_{cc}}\right)\right)\right], & x \in [0, x_1], \\ r(x_1) - (x - x_1)\tan\theta, & x \in [x_1, x_2], \\ r_{th} + r_{cc}\left[1 - \cos\left(\arcsin\left(\frac{x - x_3}{r_{cc}}\right)\right)\right], & x \in [x_2, x_3], \end{cases} \tag{C2}$$

where the positions x_1, x_2, and x_3 are defined as

$$x_1 = r_{cc} \sin \theta; \quad x_2 = x_1 + \frac{r_c - 2r_{cc}(1 - \cos \theta) - r_{th}}{\tan \theta}; \quad x_3 = x_2 + x_1. \quad \text{(C3)}$$

The supersonic part of the nozzle is obtained by mirroring the second and third sections with respect to the critical-throat position. Since the nozzle is choked, its geometry is fully defined by three parameters: the inlet Mach number $M_i = 0.08$, the arc angle $\theta = 15°$ and the arc curvature ratio $r_{cc}/r_c = 0.44$. The area ratio $A/A_* = (r/r_{th})^2$ is used to calculate the Mach number (2.1).

REFERENCES

BELL, W.A., DANIEL, B.R. & ZINN, B.T. 1973 Experimental and theoretical determination of the admittances of a family of nozzles subjected to axial instabilities. *J. Sound Vib.* **30** (2), 179–190.

DURAN, I. & MOREAU, S. 2013 Solution of the quasi-one-dimensional linearized Euler equations using flow invariants and the Magnus expansion. *J. Fluid Mech.* **723**, 190–231.

EMMANUELLI, A., ZHENG, J., HUET, M., GIAUQUE, A., LE GARREC, T. & DUCRUIX, S. 2020 Description and application of a 2D-axisymmetric model for entropy noise in nozzle flows. *J. Sound Vib.* **472**, 115–163.

GENTIL, Y., DAVILLER, G., MOREAU, S., TRELEAVEN, N.C.W. & POINSOT, T. 2024 Theoretical analysis and numerical validation of the mechanisms controlling composition noise. *J. Sound Vib.* **585**, 118463.

GOH, C.S. & MORGANS, A.S. 2011 Phase prediction of the response of choked nozzles to entropy and acoustic disturbances. *J. Sound Vib.* **330**, 5184–5198.

HUET, M., EMMANUELLI, A. & LE GARREC, T. 2020 Entropy noise modelling in 2D choked nozzle flows. *J. Sound Vib.* **488**, 115637.

JAIN, A. & MAGRI, L. 2022 A physical model for indirect noise in non-isentropic nozzles: transfer functions and stability. *J. Fluid Mech.* **925**, A33.

LE TOUZE, C., MURRONE, A. & GUILLARD, H. 2015 Multislope MUSCL method for general unstructured meshes. *J. Comput. Phys.* **284**, 389–418.

MAGRI, L. 2017 On indirect noise in multicomponent nozzle flows. *J. Fluid Mech.* **828**, R2.

MARBLE, F.E. & CANDEL, S.M. 1977 Acoustic disturbance from gas non-uniformities convected through a nozzle. *J. Sound Vib.* **55**, 225–243.

MOASE, W.H., BREAR, M.J. & MANZIE, C. 2007 The forced response of choked nozzles and supersonic diffusers. *J. Fluid Mech.* **585**, 281–304.

REFLOCH, A., *et al.* 2011 CEDRE Software (ONERA). *J. Aerospace Lab.* **2**, 1–10.

SHAPIRO, A.H. 1953 *The Dynamics and Thermodynamics of Compressible Fluid Flow*, vol. I. The Ronald Press Company.

STOW, S.R., DOWLING, A.P. & HYNES, T.P. 2002 Reflection of circumferential modes in a choked nozzle. *J. Fluid Mech.* **467**, 215–239.

TSIEN, H.S. 1952 The transfer function of rocket nozzles. *J. Am. Rocket Soc.* **22**, 139–143.

YEDDULA, S.R., GUZMAN-INIGO, J. & MORGANS, A.S. 2022 A solution for the quasi-one-dimensional linearised Euler equations with heat transfer. *J. Fluid Mech.* **936**, R3.